Turbofan Engine Control Design Using Robust Multivariable Control Technologies

Dean K. Frederick, *Life Member, IEEE*, Sanjay Garg, *Senior Member, IEEE*, and Shrider Adibhatla

***Abstract*—A unified robust multivariable approach to propulsion control design has recently been developed at National Aeronautics and Space Administration (NASA) Glenn Research Center (GRC). The critical elements of this unified approach are 1) a robust H-infinity control synthesis formulation; 2) a simplified controller scheduling scheme; and 3) a new approach to the synthesis of integrator windup protection gains for multivariable controllers. This paper presents results from an application of these technologies to control design for linear models of an advanced turbofan engine. The objectives of the study were to transfer technology to industry and to identify areas of further development for the technology to be applied by industry to the design of practical controllers for high-performance turbofan engines. The technology elements and industrial development of tools to implement the steps are described with respect to their application to a GE variable-cycle turbofan engine. A set of three-input/three-output three-state linear engine models was used over a range of power levels covering engine operation from idle to maximum unaugmented power. Results from simulation evaluation of H_∞ controller design, controller order reduction, controller scheduling, and integrator windup protection design are discussed and insight is provided into how the design parameter choices affect the results.**

***Index Terms*—Aircraft engine control, gain scheduling, H-infinity, integral windup protection (IWP), integrator windup, limit protection, multivariable control, order reduction.**

NOMENCLATURE

A8	Nozzle area.
A16	Variable bypass area.
$C(s)$	Combined actuator signal and rate.
CEPR	Core engine pressure ratio, P56/P25.
CLM	Component level model.
$E\{\cdot\}$	Expected value of $\{\cdot\}$.
IEC	Intelligent engine control.
IWP	Integrator windup protection.
J	Cost function.
$K(s)$	Controller.
$K^0(s)$	Nominal controller.
K_s	Controller output scaling matrix.
$K_{\rm IWP}$	IWP gain matrix.
LEM	Linear engine model.
LEPR	Liner engine pressure ratio, P16/P56.
MIMO	Mutliinput–multioutput.
P16	Bypass duct pressure.
P25	Compressor inlet pressure.
P56	High-pressure turbine exit pressure.
$P(s)$	Design plant.
PC	Power code.
PCN2R	Percent corrected fan speed.
PI	Proportional + integral.
PID	Proportional + integral + derivative.
RHP	Right-half of the s-plane.
$S(s)$	Sensitivity function.
SISO	Single-input, single-output.
STOVL	Short takeoff and vertical landing.
$T(s)$	Complementary sensitivity function.
$\tilde{u}$	Controller output.
$u_{\rm in}$	Scalar input to IWP design model.
$u_{\rm L}$	Actuator output after limits.
Δu	An input to IWP controller.
$U_{\rm WE}$	Weighted actuator position error.
VCE	Variable cycle engine.
WF	Fuel flow.
W_S, W_C, W_T	Weights on $S(s)$, $T(s)$, $C(s)$.
$z_{\rm in}$	Inputs to IWP design model.
$Z_{\rm WE}$	Weighted performance error.

Manuscript received March 3, 1997; revised May 2, 2000. Recommended by Associate Editor, K.Wise. This project was supported by NASA under Contract NAS3-26617. Originally published at the AIAA Joint Propulsion Conferenceand Exhibit, Lake Buena Vista, FL, July 1–3, 1996.

D. K. Frederick is with Unified Technologies, Inc., Troy, NY 12180 USA.

S. Garg is Chief of the Controls and Dynamics Technology Branch, NASA Glenn Research Center, Cleveland, OH 44135 USA.

S. Adibhatla is with the Six Sigma Group, General Electric Aircraft Engines, Evendale, OH 45215 USA.

Publisher Item Identifier S 1063-6536(00)07347-4.

I. INTRODUCTION

MOST jet engines currently in production use single input-single output (SISO) controllers, and the use of multivariable controls is a relatively new development. Current designs are often limited to two input–two output (2×2) controllers, which lend themselves to heuristic extensions of SISO methodologies for integrator windup protection. With the introduction of variable cycle engines (VCE's) of increasing complexity, as well as high-performance applications such as short takeoff and vertical landing (STOVL) systems, the need for true multivariable control methodologies is becoming apparent [1], [2].

Multivariable control research at GE Aircraft Engines initially focused on the use of Edmunds' model matching design technique [3]. Although this "KQ" model-matching technique is easy to use, it does not guarantee stability and does not take into account actuator rates. Moreover, control design over the flight envelope is achieved by designing controllers at several operating points, and scheduling the resulting gains using table-lookup schemes or curve fits (see [4]). Clearly, the use of robust control techniques to reduce gain scheduling effort and complexity is desirable.

This paper describes the application of the three steps in the unified multivariable control design approach developed at NASA's Glenn Research Center (GRC) to a set of linear models of a GE turbofan engine. The models are defined for seven power code (PC) values ranging from idle to intermediate rated power, all at sea-level standard conditions of zero aircraft speed and zero altitude. The issues that have been addressed are: 1) the design of a low-order robust H_∞ controller; 2) the application of a simplified controller-scheduling scheme; and 3) the augmentation of the multivariable controller to provide integral windup protection (IWP) when actuator saturation occurs.

The robust controller design uses variations on the standard H_∞ controller design method to include weights on actuator rates and to add extra disturbance inputs to yield controllers with improved actuator behavior and enhanced robustness to variations in the engine model parameters [5], [6]. It is anticipated that the actuator demands produced by the controller will avoid forcing the actuator servos against their rate limits during transients. The motivation for introducing disturbance inputs is to obtain a controller that results in reduced requirements for gain scheduling over the required range of flight conditions. In order to assess the robustness of the controller designed for the linear engine model at PC 35, it was used with the linear engine models for the full range of power codes (PC 20, 25, . . ., 50).

The simplified scheduling method was applied to the low-order controller designed for PC 35 to evaluate its performance at off-design operating points.

The final design method considered was directed at producing a multivariable controller that prevents integrator windup while maintaining the desired command tracking in the presence of actuator limiting [7]. The extent to which the IWP controller design approach was able to prevent integrator windup and to provide acceptable tracking of command inputs in the presence of actuator limiting was investigated by designing and simulating a IWP controller for the PC 35 controller and engine pair.

The application of these technologies to a GE turbofan engine has been described in detail by Frederick and Adibhatla [8], which forms the basis for this paper. The engine models and desired performance characteristics are first described. Then the H_∞ design process is covered, including the important issue of obtaining a low-order controller. Following a brief description of the scheduling scheme, the IWP controller design process is described and illustrated. The paper concludes with suggestions for areas in which further study is warranted in order to improve these design methods and tailor them to the needs of turbofan engine control as practiced by GE. The software tools used in this study were MATLAB and its toolboxes, Simulink, and ISICLE, which is a MATLAB toolbox written by Minto and others for use within General Electric [9]–[11].

II. Engine Models and Performance Specifications

The engine model used was the Intelligent Engine Control (IEC) [12] engine that has been employed in prior studies and for which a Fortran component-level model (CLM) and associated equilibrium-finding and linearization code were available. Because robustness and gain scheduling requirements should be an important part of any engine controller design process, seven linear engine models (LEMs) were generated that covered the power levels from idle (PC 20) to intermediate rated power (PC 50) corresponding to standard-day conditions of zero speed and zero altitude.

Each of the inputs and outputs was scaled such that a unit change in the scaled variable corresponds to approximately a 10% change in the unscaled variable. The engine inputs used in this study were fuel flow rate (WF), nozzle area (A8), and bypass duct area (A16). The controlled outputs were percent corrected fan speed (PCN2R), core engine pressure ratio (CEPR, defined as P56/P25), and liner engine pressure ratio (LEPR, defined as P16/P56). The scaled engine-model state-space matrices are listed in the Appendix.

For the design phase of this study, an actuator model consisting of three parallel unity-gain first-order lags was used. The bandwidths were taken as 26.0 rad/s for WF, 18.0 rad/s for A8, and 29.0 rad/s for A16.

Sensors were not included in the models used for design. However, for simulation purposes, the sensors were modeled as three parallel first-order lags with unity low-frequency gains and bandwidths of 50 rad/s for PCN2R and 33.3 rad/s for both CEPR and LEPR.

In addition to providing a stable closed-loop system, the primary objective of the engine controller was to give good decoupled command tracking of the demand values of PCN2R and CEPR, with good regulation of LEPR about its nominal value. Closed-loop bandwidths between 2 rad/s and 6 rad/s were considered desirable.

Because we were considering a wide range of power levels, we were particularly interested in the robustness of the controller to variations in the engine model caused by changes in power level. To provide a measure of this robustness, the step responses of the engine models were examined for the full range of power levels using the single controller designed for PC 35. When evaluating the performance of the IWP controller, our objective was to avoid windup of the integrators of the controller and to approximately track changes in the demand fan speed in the presence of actuator saturation. Exact tracking was not considered necessary because an outer control loop can be used to adjust the demand values seen by the IWP controller should saturation occur.

III. H_∞ Design

A. Design Plant

The first step in the H_∞ design process is to construct the design plant $P(s)$, as shown in Fig. 1, with the interconnections and weights selected so as to obtain the desired closed-loop characteristics when the controller is connected to the actual plant and sensors.

In a typical formulation of the H_∞ design problem, the engine and actuator models would be present, along with appropriate weights that would have been selected so as to force a controller design that would result in desired sensitivity and complementary sensitivity functions $S(s)$ and $T(s)$, respectively. As described in Garg [5] (and references therein), the typical for-

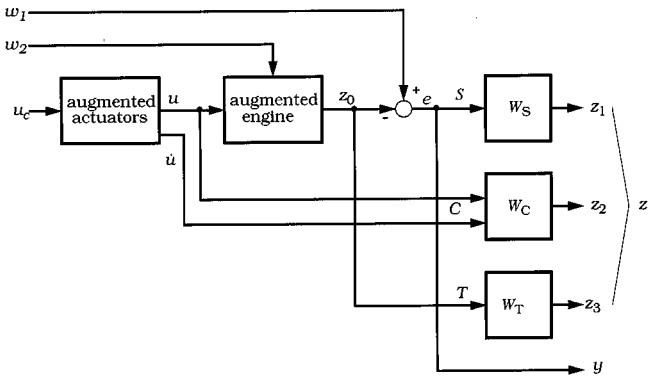

Fig. 1. H_∞ design plant $P(s)$.

mulation can be augmented in two ways in order to enhance the resulting design.

First, the actuator rates are incorporated into the $P(s)$ system, with appropriate weights to be selected by the user. This step will improve the dynamic response of the closed-loop system by eliminating high-frequency transients following a step change in demand. The only change in the design plant is the addition of three more outputs from the controller block and the corresponding weights.

The second change to the design model $P(s)$ is to add disturbance inputs to the state-variable derivatives in the engine model. The purpose of using these inputs as part of the *design* system is to synthesize a controller $K(s)$ to provide a stable closed-loop system over a wide range of power-code values.

The block named "augmented engine" represents the linear engine model with the disturbance inputs w_2 added directly to the derivatives of the engine state variables, via user-selected weights α_1, α_2, and α_3. If the linear engine model is described by the state-space matrices A, B, C, and D, with state vector x, input vector u, and output vector z_0, the state-space equations of the augmented engine model are

$$\dot{x} = Ax + Bu + \text{diag}(\alpha_1, \alpha_2, \alpha_3)w_2 \quad (1)$$

$$z_0 = Cx + Du. \quad (2)$$

The block named "augmented actuators" represents the simple actuator model of three first-order lags that produce the outputs u that drive the engine's three inputs, and three additional outputs $\dot{u}$ that are the actuator rates. The three blocks identified as W_S, W_C, and W_T are the weighting functions for the sensitivity function $S(s)$, the combined actuator and actuator rate signals $C(s)$, and the complementary sensitivity function $T(s)$, respectively.

The designer selects the weights W_S, W_T, and W_C so as to force the computational solution of the H_∞ problem to produce a controller $K(s)$ that will provide acceptable robustness, sensitivity, and performance characteristics for the closed-loop system. It is a well-known property of the H_∞ method that $K(s)$ will have the same order as $P(s)$. The engine and actuator models each have three states. If the dynamic weights $W_S(s)$ and $W_T(s)$ are each third order and W_C is constant, then both $P(s)$ and $K(s)$ will be twelthth order.

B. Weight Selections

The sensitivity weight $W_S(s)$ was chosen to be large at low frequencies in order to obtain good command tracking at low frequencies. The complementary sensitivity weight $W_T(s)$ was chosen to be large at high frequencies to obtain robustness to unmodeled high-frequency dynamics. The control weight W_C is constant and attempts to provide a controller $K(s)$ that will require reasonable actuator responses in terms of both magnitudes and rates. The sensitivity and complimentary sensitivity weights were taken to be first-order lags and leads, respectively, with the low- and high-frequency magnitudes and crossover frequencies specified by the user.

$W_S(s)$ was established as three parallel first-order lag systems having low-frequency gains of 60 dB, high-frequency gains of -60 dB, and unity-gain crossover frequencies of 2.0 rad/s. $W_T(s)$ was established as three parallel first-order lead systems having low-frequency gains of -60 dB, high-frequency gains of 60 dB, and unity-gain crossover frequencies of 8.0 rad/s. The control weights were constant values of 0.02 for each actuator.

Following the recommendations in [5], the values of α_1, α_2, and α_3 were selected on the basis of variations in the A matrix rather than the B matrix. Plots of the A matrix elements as a function of PC suggested that we should concentrate on the disturbance inputs to the first two rows. The values $\alpha_1 = \alpha_2 = 5.0$ and $\alpha_3 = 0$ were chosen based on simulation results.

Once the values of the weights had been selected, an ISICLE routine that implements the algorithm due to Safanov *et al.* [6] was used to produce the controller $K(s)$ as a set of state-space matrices.

C. Controller Design and Evaluation

The twelth-order linear controller designed for the PC 35 flight condition provided satisfactory response with the PC 35 model and stable closed-loop responses with the models for the other power conditions. Because its high order makes it impractical for implementation, the twelth-order controller was used as the basis for obtaining a reduced-order controller by using modal residualization.

Working with the twelth-order controller designed for flight condition PC 35, several different choices for the number of states to be residualized were tried. The conclusion reached was that a four-state model was the most reasonable. The poles of the fourth-order controller for PC 35 correspond to roughly three integrators and a pole at $s = -0.1476$. The reduced order controller has four finite zeros, and two of them are in the right half-plane (RHP).

The results of the reduction of the controller order from 12 to four were assessed by simulating the responses of the respective closed-loop systems to changes in demanded PCN2R and CEPR. In Fig. 2, we can see that for a unit step in PCN2R demand, there are only minor differences in CEPR and LEPR, and virtually no difference in PCN2R. On the other hand, as indicated in Fig. 3, the responses to a step change in CEPR demand do show some differences. The most important of these is the introduction of a short-duration negative transient in CEPR when the fourth-order controller was used, which suggests the pres-

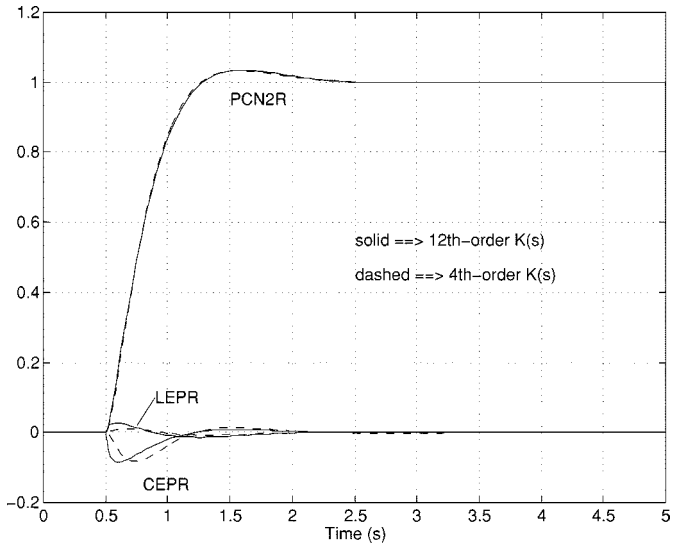

Fig. 2. Engine outputs for step in PCN2R demand with twelth-order (solid) and fourth-order (dashed) $K(s)$ at PC 35.

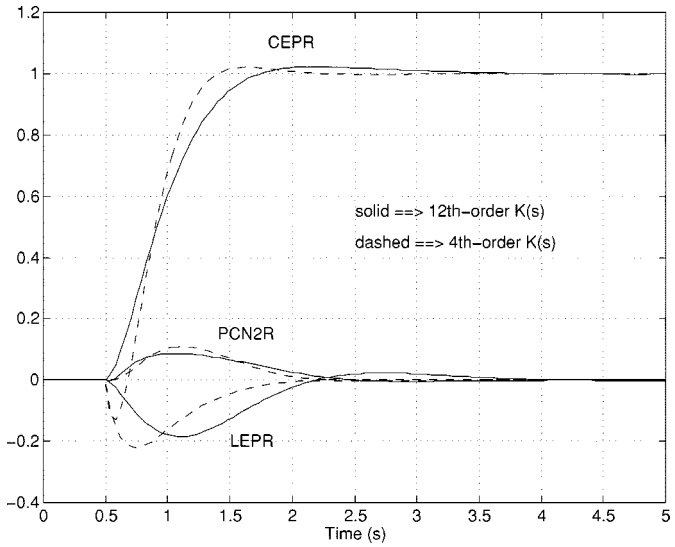

Fig. 3. Engine outputs for step in CEPR demand with twelth-order (solid) and fourth-order (dashed) $K(s)$ at PC 35.

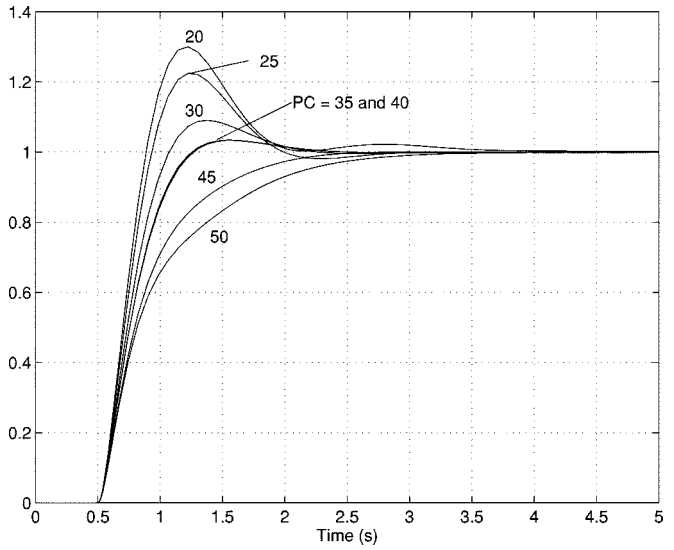

Fig. 4. PCN2R step responses for the PC 20, 25, . . ., 50 engines with fourth-order controller designed for the PC 35 engine with disturbance inputs.

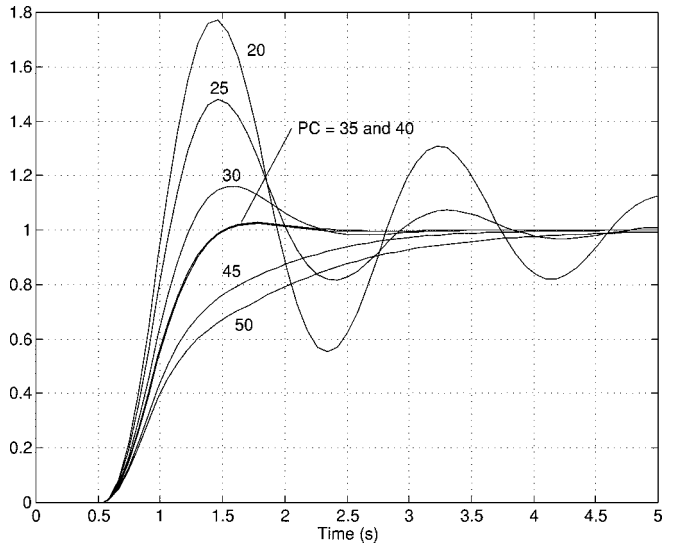

Fig. 5. PCN2R step responses for the PC 20, 25, . . ., 50 engines with fourth-order controller designed for the PC 35 engine *without* disturbance inputs.

ence of a RHP zero. This undesirable behavior was not present in the corresponding response with the twelth-order controller for which $K(s)$ had no RHP zeros. To address this issue, other methods for reducing the order of the controller should be considered, such as that of Enns [13].

To assess the robustness of the H_∞ design process, the 4th-order controller for PC 35 was used with the engine models for PC values from 20 to 50. In Fig. 4 we see the aggregate responses to a step change in demanded PCN2R. For comparison, Fig. 5 shows the responses produced with the 4th-order controller designed *without* using the disturbance inputs in the design model, which corresponds to setting $\alpha_1 = \alpha_2 = \alpha_3 = 0$ in (1). Clearly the process of using the state-rate disturbance makes the H_∞ based controller more robust to parameter variations. Although the responses with the robust controller (as in Fig. 4) are much improved over the nonrobust design, it will be necessary to provide some form of controller scheduling in order to get good step responses over the full range of PC values.

IV. Use of a Simplified Scheduling Scheme

Because a turbofan engine must perform over a wide range of operating conditions, the traditional control-design approach is to perform linear designs at a number of operating points and then to schedule the numerical parameters of the control law according to a curve fitting algorithm. One of our objectives in applying the H_∞ control-design methodology is to reduce the scheduling demands so a simpler-than-usual scheduling scheme can be used. As a very preliminary look at this important aspect of engine control design, we have applied a technique recently developed by Garg [14] for providing simplified scheduling for multivariable controllers.

The step responses in Fig. 4 show that the single fourth-order H_∞ controller designed for PC 35 is capable of controlling all seven linear engine models for the full range of power codes in a stable manner. However, with the exception of the two responses for the PC 35 and PC 40 engines, which are almost identical, these responses are not satisfactory, due to excessive overshoot or slow response. Clearly, the PC 35 controller requires some form of scheduling in order to provide satisfactory responses over the full range of power codes.

The scheduling method applied here considers the scheduled controller $K(s)$ as

$$K(s) = K_s K^0(s)$$

where K_s is the controller output-scheduling matrix, which is dependent on the engine's operating point, and $K^0(s)$ is the nominal controller. For our example, we consider the fourth-order PC 35 controller to be the nominal one so engine models with PC values other than 35 represent off-nominal conditions.

The controller-output scheduling matrix is 3×3, thus requiring nine parameters to be scheduled as a function of the power code. As a comparison, a fourth-order multivariable controller with three inputs and three outputs will require up to 49 parameters to be scheduled, while, for a 3×3 proportional-plus-integral (PI) controller, 18 parameters must be scheduled.

An optimization problem was created for each off-nominal operating point in which the scheduling matrix K_s was computed so as to minimize the infinity norm of the normalized loop transfer difference between the nominal control loop (PC 35) and the off-nominal control loop (corresponding to other power conditions). For each of the seven power codes, the MATLAB Optimization Toolbox was used to compute the output scheduling so as to minimize a related cost function over a set of frequencies covering the frequency range of interest.

When the closed-loop system with this scheduling scheme was simulated for step changes in demanded PCN2R, the responses shown in Fig. 6 were obtained for the power codes ranging from 30 to 50. Because the controller was designed for the PC 35 engine and because the response for the PC 40 engine with the PC 35 controller has been shown to be virtually identical to the response for the PC 35 engine, there is no need for scheduling at either PC 35 or PC 40, which means that the gain matrix is the identity matrix for both of these power codes. As seen in comparison with Fig. 4, the simplified scheduling provides much improved performance over the nonscheduled controller for power codes 30, 45, and 50.

The scheduling gains calculated for the idle and close-to-idle conditions of PC 20 and 25 did not provide acceptable step responses, so those two power codes have not been included in Fig. 6. Examination of the A matrices for the linear engine models at these two lowest power codes revealed a pair of complex open-loop eigenvalues, whereas the eigenvalues are all real for the linear engine models at the other power codes. The engine used for this study contains a bypass door that is open for lower power codes (PC 20 and 25) and closed for PC values of 30 and above. Hence, it appears that the scheduled PC 35 controller can be used in the single-bypass regime ($30 \leq \text{PC} \leq$ 50), while another controller will need to be designed for the double-bypass regime ($20 \leq \text{PC} < 30$).

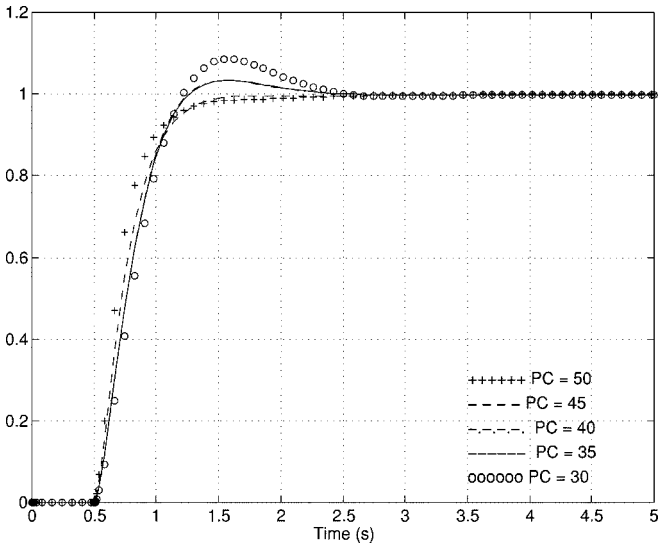

Fig. 6. PCN2R step responses for engines PC 30, . . ., PC 50 with fourth-order controller designed for the PC 35 engine and controller-output scheduling.

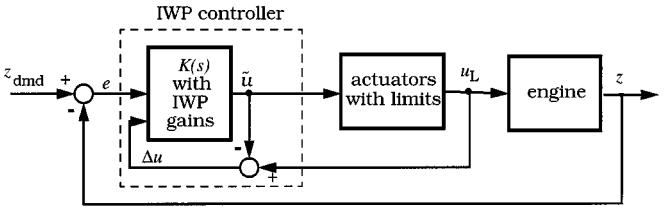

Fig. 7. Nonlinear closed-loop system, with limiting and IWP controller.

V. Integrator Windup Protection

Watts and Garg [7] have developed a heuristic methodology for the design of MIMO integrator windup protection (IWP) controllers that shows promise for the control of jet engines. In this section, we discuss the application of this design method to the GE linear engine model for PC 35 that was used in the H_∞ controller study, but with actuator limiting present.

A. Controller Structure

The design procedure consists of developing three design models, one for each actuator. Each design model is used to compute a column vector of IWP gains for the particular actuator under consideration that will minimize the cost for a heuristically-defined optimization problem. Then the individual IWP gain vectors, one per actuator, are combined to form the IWP gain matrix which is used to modify the output of the original state-space controller only when one or more of the actuators is being limited because of hardware constraints or operational limits.

The nonlinear feedback system shown in Fig. 7 is assumed to have saturation limits on the actuators and has an IWP controller. The controller output $\tilde{u}$ is subtracted from the actuator output $u_{\rm L}$, that may at times be limited, to form the second input to the IWP controller, Δu. If the actuators are not limited and the actuator dynamics are not a factor, then $u_{\rm L} = \tilde{u}$ so $\Delta u = 0$.

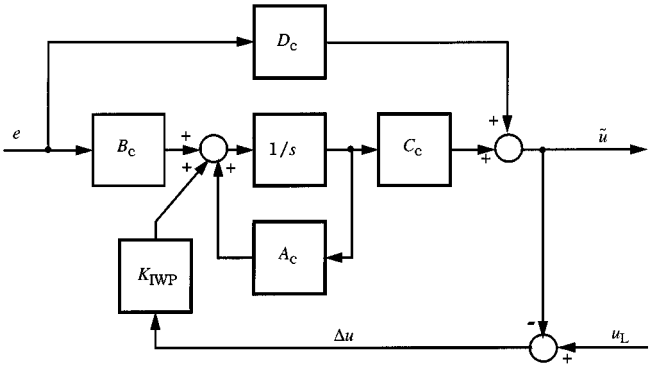

Fig. 8. Details of the IWP controller.

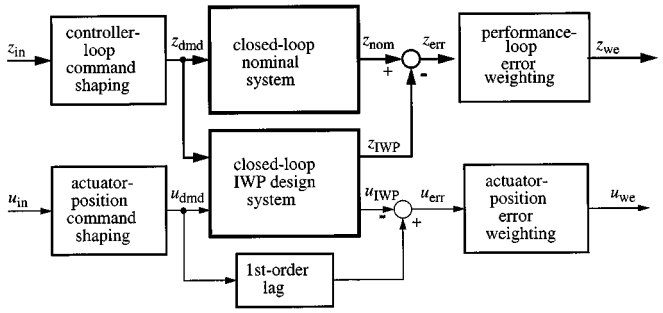

Fig. 9. Design model.

Fig. 8 shows the detailed form of the IWP controller. In particular, we have a conventional linear state-space controller whose state-variable derivative vector is augmented by the term $K_{\mathrm{IWP}}\Delta u$, where the three-element vector Δu is a measure of the amount of limiting in each actuator. With the assumption that we have a specific linear controller $K(s)$, the only element in the IWP controller that remains to be determined is the gain matrix K_{IWP}. This matrix has one column for each actuator and n rows, where n is the number of state variables in the controller. The elements of K_{IWP}, which are constants dependent on the flight condition, are determined one column at a time by solving a nonlinear minimization problem.

The cost function to be minimized is the expected value of the sum of weighted tracking and actuator errors generated by a linear *design* model. Once the gain vector for one actuator has been determined, a similar design model is constructed for the next actuator and the optimization process is repeated. Because our engine has three actuators, the process is done three times to obtain the $n\times 3$ matrix K_{IWP}, where n is the number of states in the reduced order controller. Although the design method can be extended to account for the simultaneous saturation of multiple actuators, the methodology described here assumes that only one actuator is saturated at a time. However, as demonstrated in the later sections, the IWP gains synthesized with single actuator saturation at a time performed adequately when simultaneous saturation of multiple actuators was encountered during simulation evaluations.

B. Problem Formulation for IWP Gain Synthesis

Fig. 9 shows the top-level structure of the design model, the main elements of which are the two blocks labeled "closed-loop nominal system"' and "closed-loop IWP design system." The external inputs, z_{in}, a three-element vector, and the scalar u_{in}, are white-noise signals that are filtered so as to provide tracking- and actuator-demand signals that have appropriate weighting and frequency spectra. The upper main block represents the linear closed-loop system, which consists of the engine, the actuators *without limiting*, and the linear controller $K(s)$. The response of this nominal system is what we would obtain if actuator limiting did not occur. As such, the nominal system represents what we would like to obtain in the presence of limiting, but might not be able to. The heavy lines into and out of the block represent vector signals having three elements each.

The lower main block in Fig. 9 represents the closed-loop IWP design system for a specific actuator. For discussion purposes, we will use the fuel flow actuator, whose output is WF. Note that this block has two inputs and two outputs. The upper input (the thicker of the two) is the same three-element vector received by the nominal system, and represents the frequency-shaped demand inputs to be tracked by the closed-loop system (PCN2R, CEPR, and LEPR). The lower input (the thinner of the two) is a scalar that represents the frequency-shaped actuator signal for which the IWP gains are being determined. In this case it is the demanded fuel flow rate $\mathrm{WF}_{\mathrm{dmd}}$.

Watts and Garg [7] also include magnitude scale factors and the corresponding inverse scale factors on the plant outputs in their design model. However, all of the variables associated with the GE engine model have been scaled, so no further scaling was required.

The design model of Fig. 9 is considered to be driven by white noise and the weighted performance error and the weighted actuator error are dependent on the values of the IWP gain vector for the actuator under consideration. Hence, the IWP gain vector is determined so as to minimize the cost J defined as

$$J = \mathrm{E}\left\{\lim_{T\to\infty}\frac{1}{T}\int_0^T (Z'_{\mathrm{WE}}Z_{\mathrm{WE}} + U^2_{\mathrm{WE}})\,dt\right\} \qquad (3)$$

where E denotes "expected value of" and $'$ denotes transpose.

This optimization problem can be solved by using a compatible set of computer tools to do the following:

- implement the design model represented in Fig. 9 for the specific actuator whose IWP gains are being determined;
- create a function that will use the design system to compute the cost J for a specified IWP gain;
- use a suitable optimization routine to perform the nonlinear minimization.

The process described above is repeated, with appropriate modifications to the design plant, to produce the IWP gain vector for each of the three actuators. These three gain vectors are then combined to form the IWP gain matrix, so the final controller appears as shown in Fig. 8, where all of the signals are vectors.

When the IWP gains were computed for the GE engine under consideration, so as to minimize the cost J expressed in (3), it turned out that a minimum of the cost could not be found for gains of any reasonable magnitude. The optimization routine, which imposed no constraints on the magnitude of the gain

vector, was able to continue reducing the cost slightly by increasing the gain manitude. It was verified via simulation that these large-gain solutions did indeed produce stable closed-loop systems, but they were certainly not desirable. In order to obtain solutions with reasonable magnitudes, the term $0.2\sqrt{K'K}$, which is proportional to the magnitude of the IWP gain vector K, was added to the cost defined by (3), With this modification, solutions that had reasonable gains and produced satisfactory responses were obtained.

C. IWP Gain Calculation and Evaluation

A Simulink implementation of the design system shown in Fig. 9 was used to determine the IWP gains for limiting of the fuel flow (WF). Then the process was repeated with the design systems for limiting of the nozzle area (A8) and of the variable bypass area (A16) to obtain the remaining two sets of gains.

To ensure that an acceptable minimum had been found, the optimization process was repeated from several starting points in the four-dimensional gain space. If an initial choice resulted in an unstable closed-loop system, it was discarded and another starting point selected. If all of the stable starting points resulted in terminal points that were reasonably close to one another in the gain space, with final values of the cost that were approximately the same, then the minimum found was deemed to be acceptable.

The IWP gain matrix for the PC 35 flight condition was obtained by combining the three four-element gain vectors into a 4×3 matrix gain matrix K_{IWP} shown in Fig. 8. The first column contains the gains that are active when WF limits, the second column the gains for A8, and the third column the gains for A16. At this point, the design was complete.

The evaluation of the IWP controller was carried out using Simulink. For the simulation runs, somewhat arbitrary values of ± 1.5 units were used for each pair of actuator limits (recall that all actuator values were scaled). The input signal employed for all of the tests was a rectangular pulse in demanded PCN2R, starting at $t = 0.5$ s and ending at $t = 4.0$ s. Such a finite-duration pulse will make the effects of any integrator windup apparent, should they occur. The pulse amplitudes were selected to achieve different degrees of limiting, as described below.

Three sets of tests were run. First, the H_∞ controller without IWP was used, with limiting possible on all three actuators. Then, the IWP controller was used, again with limiting on all three of the actuators. Finally, a set of runs was done both with and without the IWP controller, with limiting only on A8 and A16. For all cases, the engine model and the fourth-order H_∞ controller were those for the PC 35 operating condition.

The fan speed responses (PCN2R) for pulses in PCN2R demand of 1.0, 1.5, 2.0, and 3.0 units without any IWP control appear in Fig. 10. For a pulse height of 1.0 unit, which corresponds to a change of 10% in demanded PCN2R, no limiting occurs. Hence, the response for the first 4.0 s is the same as that shown in Fig. 2.

When the height of the input pulse is increased to 1.5 units, the fuel flow actuator (WF) is forced against its limit, and the nozzle actuator (A8) is limited for a portion of the duration of the input pulse. The rise in PCN2R is a bit slower than for the linear response, but the tracking for PCN2R is still good, with no steady-state error.

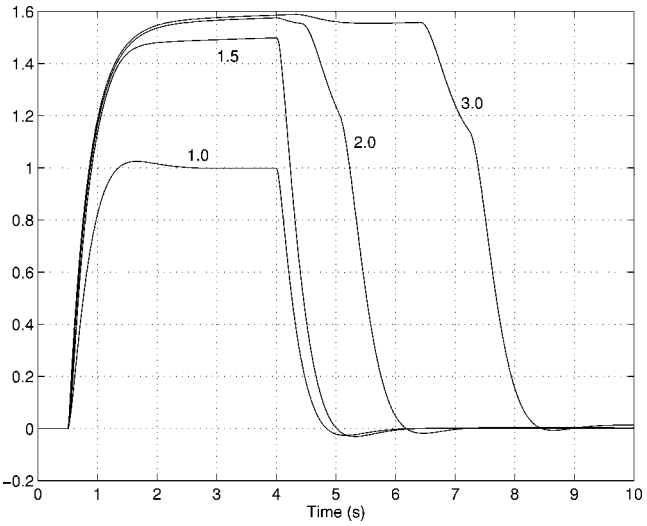

Fig. 10. PCN2R responses, without IWP control to pulses in demanded PCN2R, with limiting on all three actuators.

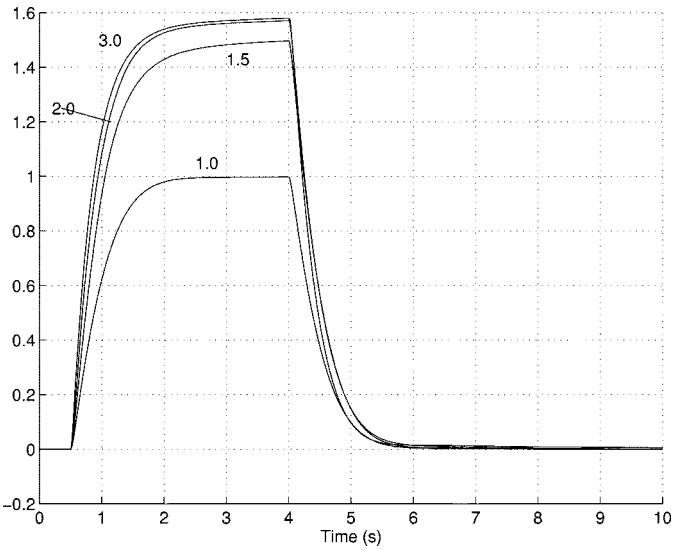

Fig. 11. PCN2R responses, with IWP control to pulses in demanded PCN2R, with limiting on all three actuators.

For a pulse height of 2.0 units in demanded PCN2R, both WF and A8 limit hard, and WF remains on its limit well after the input pulse has ended. The fan speed response is no longer able to track its demanded input and exhibits a clear indication of integrator windup.

When the input pulse height is increased to 3.0 units, the amount of windup increases further, and all three actuators become limited. The A8 actuator remains limited until $t = 6.4$ s and the fuel flow actuator (WF) is limited until $t = 7.4$ s. Clearly, these latter two responses are unsatisfactory and suggest that IWP control is essential for acceptable performance in the presence of actuator limiting.

In Fig. 11 we see the results of performing the same set of four runs described above, but with the IWP controller active.

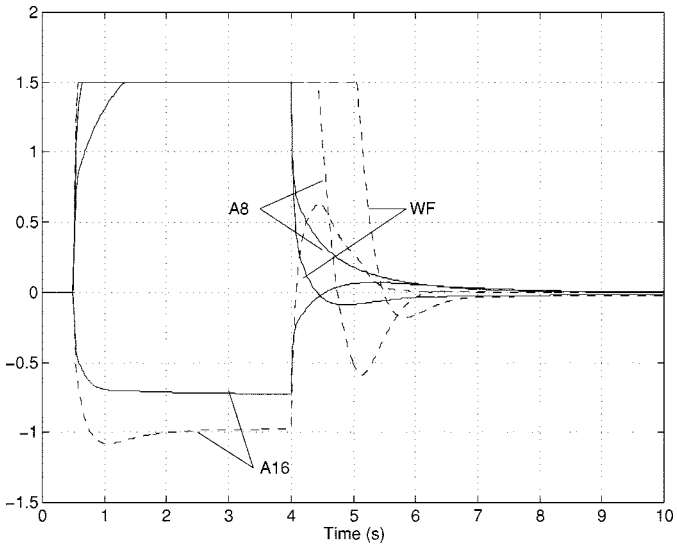

Fig. 12. Actuator responses for pulse height of 2.0, with (solid) and without (dashed) IWP control.

By comparing these curves with those in Fig. 10, we are led to the following three conclusions. First, and most important, the integrator windup that seriously impaired the responses in Fig. 10 was eliminated by the IWP controller. Second, as noted from Fig. 11, the IWP gains did not improve the capability of the system to track steady-state commands for the pulses of height 2.0 and 3.0.

The third observation is that the two responses for a pulse height of 1.0 (in Figs. 10 and 11) are not the same, although there was no actuator limiting in either of these runs. This was because actuator dynamics caused Δu to the IWP controller to be nonzero, even in the absence of limits. This effect can be eliminated by including a dynamic model of the actuators in the path going from the controller controller output $\tilde{u}$ to the summing junction that forms Δu.

Because the corrected fan speed (PCN2R) is a good measure of the thrust produced by the engine, it is essential that the demanded values of PCN2R be met in the steady state, provided that no operational constraints such as high temperatures or pressures are being violated. The primary reason that the system is unable to track PCN2R demand for pulses of height greater than 1.5 units is that the fuel flow (WF) becomes limited. A final set of tests was run without any limiting on WF, in order to evaluate the effects of the IWP controller with only A8 and A16 limited.

These tests showed that without any limiting on fuel flow, the ability of the controller to track the demanded fan speed was improved considerably. However perfect steady-state tracking of the corrected fan speed, as in the nominal case with no actuator limits, was still not achieved.

As a final demonstration of the benefits of the IWP controller, Fig. 12 shows the responses of the three actuators (fuel flow, nozzle area, and bypass duct area) corresponding to a pulse height of 2.0 units in PCN2R demand. The solid lines, which result from using the IWP controller, all begin returning to their equilibrium values of zero immediately upon termination of the input pulse, thereby indicating an absence of windup. On the other hand, the dashed lines (no IWP control) for WF and A8 continue at their saturated values of 1.5 for some time after the end of the pulse, and all three actuators undergo oscillatory transients before settling to zero.

VI. Discussion

The results presented in the previous sections have shown that the three steps in the robust multivariable control design approach lead to satisfactory performance for an advanced propulsion system with reasonable low order controllers which require minimal scheduling and accommodate the effect of actuation limits with minimal performance degradation. However, the results also showed some shortcomings of the design approach which will need to be addressed for this approach to be acceptable to practicing control engineers in the industry. Some future research areas which can help address these shortcomings are summarized in the following.

The reduced-order controller transfer function discussed in Section III C had two zeros in the right half of the s-plane, and resulted in a negative dip at the beginning of the CEPR step response. Other order-reduction methods, such as the frequency-weighted model reduction scheme of Enns [13], should be investigated as a possible way of obtaining a reduced order controller that does not have a right half-plane zero. As discussed in Section IV, the simplified scheduling scheme was not able to provide satisfactory closed-loop performance for the low power conditions (PC20 and PC25). It was noted that the fundamental dynamic behavior of the engine was different at these power levels due to the way the engine is operated at these conditions. There is a need to develop a systematic approach to provide guidance to the control designer in determining what region of operation around an operating point can be covered by using the simplified scheduling scheme in conjunction with a robust controller designed for the operating point. As discussed in Section V, the IWP scheme did not provide perfect steady-state tracking of the corrected speed when limits on A8 and A16 were encountered while the fuel flow was not being limited. Modifications to the IWP gain design approach need to be developed to ensure that perfect steady-state tracking of a controlled variable can be maintained if the primary effector for controlling that variable is not being limited. Whether this can be accomplished simply by adjusting the weights in the performance index for synthesizing the IWP gains, or whether other modifications will be needed remains to be seen.

Because rate limits and rate-like limits (acceleration and deceleration schedules, for example) are of special importance to engine control applications, it is also desirable to adapt the IWP scheme to handle rate limits rather than just saturation limits. In addition, the IWP design methodology should be compared to the nominal integrator windup protection currently used at GE Aircraft Engines, and to other techniques that "condition" the controller states, such as those of Hanus [15], [16]. Such a comparison should be made on the basis of performance as well as ease of design and implementation, which affect development cost.

VII. Conclusion

Simulation results have shown that the linear reduced order H_∞ controller designed with actuator rates and disturbance inputs included in the design model was able to provide good responses to step changes in demanded fan speed and core engine pressure ratio that avoided discontinuities in the demand signals to the actuators. Simulations also verified that a single fourth-order controller designed for partial power was able to provide stable responses for linear sea-level, standard engine models at power levels ranging from idle to maximum unaugmented power, without any scheduling. The use of a simplified output matrix gain scheduling scheme for this single low-order controller yielded good step responses for power codes ranging from 30 to 50. Finally, it has been demonstrated that the low-order H_∞ controller can be augmented so as to avoid integrator windup when one or more of the actuators is forced against its limit. Areas of future research have been identified which will make the techniques presented in the paper more appealing to practicing engine control designers in the industry.

Appendix

The state-space matrices of the linearized engine model for PC 35 are

$$A_{\text{eng}} = \begin{bmatrix} -4.1476 & 1.4108 & 0.0633 \\ 0.2975 & -3.1244 & 0.0623 \\ -0.0429 & -0.1729 & -0.1325 \end{bmatrix}$$

$$B_{\text{eng}} = \begin{bmatrix} 0.2491 & 0.0969 & -0.0112 \\ 0.2336 & 0.0335 & 0.0047 \\ 0.0624 & 0 & 0 \end{bmatrix}$$

$$C_{\text{eng}} = \begin{bmatrix} 8.7379 & 0 & 0 \\ -3.3033 & 3.8052 & 0.0542 \\ 2.1940 & -2.5749 & -0.0295 \end{bmatrix}$$

$$D_{\text{eng}} = \begin{bmatrix} 0 & 0 & 0 \\ 0.2383 & -0.2748 & 0.0224 \\ -0.1455 & 0.0580 & -0.2293 \end{bmatrix}.$$

Acknowledgment

The authors would like to thank C. Resnick of GE Aircraft Engines, D. Minto of GE Power Systems, and R. Rajamani of GE Corporate Research and Development for their assistance.

References

[1] S. W. Kandebo, "GE eyes variable cycle for engine competition," *Aviation Week Space Technol.*, Mar. 29 1993.

[2] S. Adibhatla, "Propulsion control law design for the NASA STOVL controls technology program," in *Proc. AIAA 93-4842, AIAA Int. Powered Lift Conf.*, Santa Clara, CA, Dec. 1–3, 1993.

[3] J. M. Edmunds, "Control system design and analysis using closed-loop nyquist and bode arrays," *Int. J. Contr.*, vol. 30, no. 5, pp. 773–802, 1979.

[4] J. A. Polley, S. Adibhatla, and P. J. Hoffman, "Multivariable turbofan engine control for full flight envelope operation," presented at the Gas Turbine and Aeroengine Congress and Exposition, Amsterdam, The Netherlands, June 5–9, 1988, ASME Paper 88-GT-6.

[5] S. Garg, "Robust integrated flight/propulsion control design for a STOVL aircraft using H_∞ control design techniques," *Automatica*, vol. 29, no. 1, pp. 129–145, 1993.

[6] M. G. Safonov, D. J. N. Limebeer, and R. Y. Chiang, "Simplifying the H_∞ theory via loop-shifting, matrix pencil and descriptor concepts," *Int. J. Contr.*, vol. 50, no. 6, pp. 2467–2488, 1989.

[7] S. R. Watts and S. Garg, An optimized integrator windup protection technique applied to a turbofan engine, , NASA Lewis Research Center, Cleveland, OH, 1994.

[8] D. K. Frederick and S. Adibhatla, "The application of H_∞ and integrator windup protection control design algorithms to a GE turbofan engine,", Final Rep. NASA Lewis Large Engine Technology (LET) Task Order 58, Contract NAS3-26 617, Dec. 1995.

[9] A. Grace, A. Laub, J. Little, and C. Thompson, *Control System Toolbox for Use with MATLAB*. Natick, MA: The MathWorks, Inc., 1992.

[10] A. Grace, *Optimization Toolbox for Use with MATLAB*. Natick, MA: The MathWorks, Inc., 1992.

[11] K. D. Minto, *ISICLE Tutorial User's Guide*. Schenectady, NY: Contr. Syst. Lab., GE-CRD, 1993.

[12] S. Adibhatla, H. Brown, and Z. Gastineau, "Intelligent engine control (IEC)," in *AIASA 92-3484, 28th Joint Propulsion Conf. Exhibit*, Nashville, TN, July 6–8, 1992.

[13] D. F. Enns, "Model reduction for control system design," Ph.D. dissertation, Dept. Aeronautics Astronautics, Stanford Univ., Stanford, CA, 1984.

[14] S. Garg, "A simplified scheme for scheduling multivariable controllers and its application to a turbofan engine," presented at the Int. Gas Turbine Aeroengine Congr Exhibition, Birmingham, U.K., June 1996, ASME Paper 96-GT-104.

[15] R. Hanus, "A new technique for preventing control windup," *J. A*, vol. 21, no. 1, pp. 15–20, 1980.

[16] R. Hanus, M. Kinnaert, and J. L. Henrotte, "Conditioning technique, A general anti-windup and bumpless transfer method," *Automatica*, vol. 23, no. 6, pp. 729–739, Nov. 1987.

Dean K. Frederick (S'60–M'64–LM'00) received the B.E. degree in mechanical engineering at Yale University, New Haven, CT, in 1955, the Sc.M. degree at Brown University, Providence, RI, in 1961, and the Ph.D. degree in electrical engineering at Stanford University, Stanford, CA, in 1964.

He was a faculty member in the Department of Electrical, Computer, and Systems Engineering, Rensselaer Polytechnic Institute, Troy, NY, for 30 years, retiring in 1994. Since then, he has spent the majority of his time working on jet engine control problems for General Electric Aircraft Engines and for the GE Corporate Research and Development Center in Niskayuna, NY. He has coauthored three books dealing with the modeling, analysis, and control of dynamic systems.

Sanjay Garg (M'89–SM'91) received the B.Tech degree in aeronautical engineering from Indian Institute of Technology, Kanpur, India, the M.Sc. degree in aerospace engineering from University of Minnesota, Minneapolis, and the Ph.D. degree in aeronautics from Purdue University.

He is currently the Chief for the Controls and Dynamics Technology Branch at NASA Glenn Research Center, Cleveland, OH. His research interest is in all aspects of applications of multivariable control technologies to aerospace vehicles with emphasis on propulsion control and active control of propulsion system components.

Dr. Garg is an Associate Fellow of AIAA and a past member of the AIAA Technical Committee on Guidance, Navigation, and Control. He served as the Technical Program Chairman for the 1993 AIAA Guidance, Navigation and Control Conference and as Associate Editor for the AIAA Journal of Guidance, Control and Dynamics from 1994 to 1996.

Shrider Adibhatla received the Bachelor's degree in mechanical engineering from the Indian Institute of Technology, Kanpur, India, in 1976, and the Ph.D. degree in mechanical engineering from the University of Kentucky, Lexington, in 1981.

After working for four years at the Kentucky Center for Energy Research on the clean combustion of coal, he joined GE Aircraft Engines. At GE, he worked in the Advanced Controls group, specializing in model-based control and diagnostics, integrated flight and propulsion control, and multivariable control of variable-cycle engines. He also managed Air Force and NASA programs to transition model-based and multivariable controls technologies to military and commercial jet engines. He is currently a Black Belt in the engineering division of GE's six-sigma program.